Effect of confining walls on the interaction between particles in a nematic liquid crystal

Effect of confining walls on the interaction between particles in a nematic liquid crystal

Jun-ichi Fukuda[1]**, Bohdan I Lev**[1,2] **and Hiroshi Yokoyama**[1,3]

[1] Yokoyama Nano-structured Liquid Crystal Project, ERATO, Japan Science and Technology Corporation, 5-9-9 Tokodai, Tsukuba 300-2635, Japan
[2] Department of the Theoretical Physics, Institute of Physics, NAS Ukraine, Prospekt Nauki 46, Kyiv 04022, Ukraine
[3] Nanotechnology Research Institute, AIST, 1-1-4 Umezono, Tsukuba 305-8568, Japan

E-mail: fukuda@nanolc.jst.go.jp

Abstract

We investigate theoretically how the confining walls of a nematic cell affect the interaction of particles mediated by the elastic deformation of a nematic liquid crystal. We consider the case where strong homeotropic or planar anchoring is imposed on the flat parallel walls so that the director on the wall surfaces is fixed and uniform alignment is achieved in the bulk. This set-up is more realistic experimentally than any other previous theoretical studies concerning the elastic-deformation-mediated interactions that assume an infinite medium. When the anchoring on the particle surfaces is weak, an exact expression of the interaction between two particles can be obtained. The two-body interaction can be regarded as the interaction between one particle and an infinite array of 'mirror images' of the other particle. We also obtain the 'self-energy' of one particle, the interaction of a particle with confining walls, which is interpreted along the same way as the interaction of one particle with its mirror images. We show that the walls play a different role in homeotropic and planar cells, which is attributed to the difference in the symmetry of the cells. We also present the landscapes of the interaction energy when one particle is fixed and demonstrate that the interaction is sensitively dependent on the fixed particle as well as the interparticle distance.

1. Introduction

Liquid crystal colloids and emulsions [1–7] have attracted considerable interest during the last few years as a different class of composite material from conventional colloids [8]. One of the interesting and fascinating properties of liquid crystal colloids is that the anisotropy of the host liquid crystal and its spatial variation, or the elastic deformation of liquid crystal ordering, can

mediate interaction between particles or droplets immersed in it [9]. Such interactions, which are of course absent in usual colloids with isotropic host fluids, have proven to yield various kinds of superstructures formed by particles, including linear chains [2, 10–12], anisotropic clusters [1, 13] and periodic lattices [14]. Similar arguments also hold for structure formation by inclusions in two-dimensional smectic C films, and several experimental observations of chain-like structures [15, 16] and two-dimensional lattices [16] have been reported. The variety of these superstructures, some of which are unique to liquid crystal colloids and have not been observed in other colloidal systems, has been not only of academic interest but also of technological importance, because they provide a different possibility of controlling the morphology of a colloidal system because a liquid crystal is easily tunable by varying the temperature or applying external fields. We notice that recently there have been reports of several experimental attempts to change the droplet superstructures in a nematic liquid crystal by external perturbations such as an electric field [17], a magnetic field [18] or light emission with the aid of photochromic azobenzene derivatives [19].

The elasticity-mediated interaction in a liquid crystal has been one of the important challenges in liquid crystal science because it is crucial in understanding what structures will be observed in what conditions in liquid crystal colloids. Poulin *et al* [9] measured this interaction experimentally by observing the viscously damped motion of two droplets in a nematic liquid crystal [9]. Several theoretical studies based on analytical arguments and numerical calculations have been devoted to the understanding of the particle interaction in a liquid crystal. One of the pioneering studies was carried out by Lopatnikov and Namiot [20], who showed analytically that the interaction potential U between cylindrical particles in a nematic liquid crystal is of an anisotropic dipole–dipole form that behaves as $U \sim r^{-3}$, with r being the interparticle distance. Later, Ramaswamy *et al* [21] and Ruhwandl and Terentjev [22] found that when the surface anchoring is so weak that the elastic deformation is also weak enough, spherical particles exhibit a quadrupole–quadrupole interaction ($U \sim r^{-5}$) in a nematic liquid crystal. Lubensky *et al* [23] showed by a phenomenological argument that particles carrying a hedgehog defect act as 'dipoles' and the interaction between such dipoles is responsible for the chain-like structure of particles observed in experiments [2, 10, 11]. This dipole interaction was also confirmed by numerical calculations [24]. Lev and co-workers [25–27] developed a general theoretical framework that can be applied to particles with arbitrary shapes. One of their important conclusions is that the form of the interaction is closely related to the symmetry of the particles themselves or that of the regions around the particles with strong elastic deformation, which the authors referred to as the 'coat'. They argued that even Coulomb-type interaction ($U \sim r^{-1}$) would be possible when only one symmetry plane exists around the particle [27]. We also point out that the symmetry of the host liquid crystal is of course an important factor, and although many of the theoretical studies concern nematic liquid crystals as mentioned above, smectic [20, 28, 29], cholesteric [30] and paranematic [31–33] (above the nematic–isotropic transition) liquid crystals and two-dimensional films [34, 35] have also been discussed as host fluids.

However, almost all of the previous theoretical studies concerning the interaction of particles in liquid crystals have treated a background liquid crystal as an infinite medium. In actual experiments, on the contrary, liquid crystals are confined in a cell or container, whose walls may affect the interaction between particles because they limit the modes of the elastic deformation of liquid crystals. Moreover, the walls themselves can interact with the suspended particles via liquid crystals. Therefore the confining walls may have an important effect on the particle interactions and the resultant superstructures formed by particles. So far as we know, the only theoretical study which has dealt with interaction in a finite liquid crystal is our previous study [36]. There we discussed the interaction in a hybrid nematic cell, where

one of the confining walls imposes homeotropic anchoring and the other planar (or tangential) anchoring, thus leading to non-uniform orientation of the nematic liquid crystal. We have shown that the interaction between particles in a hybrid nematic cell is highly complex and significantly different from that in a uniform nematic, which all of the previous theoretical studies have dealt with. The complexity of the interaction potential arises not only from the initial deformation of the host nematic but also from the confinement, due to which only those modes of the elastic deformation of liquid crystals with discrete wavenumber are allowed.

Considering the gap between the possible relevance of the effect of confining walls in actual experiments and the lack of theoretical understanding of it, we believe that it is worthwhile giving a detailed discussion of the effect of confinement on the elasticity-mediated interaction between particles in a uniform nematic liquid crystal, which is the aim of this paper. The theoretical technique developed in our previous studies can also be applied to this problem, which allows an analytical treatment of the problem to yield an exact expression of the interaction energy in the case of weak anchoring on the particle surfaces. We deal with a uniformly aligned cell in contrast to our previous study [36], and the absence of any initial deformation in a nematic liquid crystal makes it clear how the confining walls affect the interaction of particles immersed in the nematic cell. We will show that the confining walls act as 'mirrors' and the interaction between two particles can be interpreted as that between one particle and the infinite array of mirror images of the other. Moreover, the self-energy of one particle, which is considered as the interaction of a particle with confining walls, can also be regarded as the interaction between the particle and its mirror images. We will also show that the form of the interaction energy in a homeotropically aligned cell and that in a planar cell are essentially different; this is attributed to the difference in the symmetry of the cell.

In section 2, we present the resultant form of the interaction energy and the self-energy together with a theoretical treatment of the problem. Section 3 is devoted to a discussion of the implication of the results given in 2. Section 4 gives a brief conclusion.

2. Calculation of the free energy

In this section we calculate the total elastic energy of a nematic cell containing particles. In section 2.1 we give a detailed formulation of the problem in the case of a homeotropically aligned nematic cell. The theoretical treatment in section 2.1 can also be directly applied to the case of a planar nematic cell, which will be presented in section 2.2.

2.1. Formulation of the problem (homeotropic anchoring case)

We prepare a nematic liquid crystal confined between two parallel walls a distance d apart. Strong homeotropic anchoring is imposed on each of the two walls so that the nematic liquid crystal takes a uniform alignment perpendicular to the walls. For simplicity we assume that the anchoring is strong enough for the director on the confining surfaces to be fixed. We set the z-axis perpendicular to the walls (or parallel to the initial alignment of the liquid crystal) and let the two walls be represented by $z = 0$ and d. To simplify the following calculations we assume the one-constant approximation for the Frank elastic energy, which is then given by [37, 38]

$$F_b = \tfrac{1}{2}K \int d^2 r_\perp \int_0^d dz \, \{(\nabla \cdot n(r))^2 + (\nabla \times n(r))^2\}, \tag{1}$$

where K is the elastic constant, $r_\perp = (x, y)$ and $n(r)$ is the director specifying the local orientation of the nematic liquid crystal at r. Since $|n| = 1$, n can be written as

$n = (n_x, n_y, 1 - \mathcal{O}(n_x^2 + n_y^2))$. Here we further assume that the director distortion (n_x, n_y) due to the inclusion of particles in the nematic cell is small enough, so that the elastic energy (1) can be expanded in terms of n_x and n_y. This assumption can be justified when the anchoring on the particle surfaces is weak enough, and a detailed discussion on the condition of weak anchoring will be given below. When we retain terms up to second order in n_x and n_y, we have

$$F_b = \frac{1}{2} K \int d^2 r_\perp \int_0^d dz \, \{(\nabla n_x(r))^2 + (\nabla n_y(r))^2\}. \tag{2}$$

For clarity of the discussion below, we introduce the Fourier transform of n_x and n_y. Since we have assumed strong anchoring on the wall surfaces, $n_{x,y}(z=0) = n_{x,y}(z=d) = 0$. The definition of the Fourier transform consistent with this constraint is

$$n_{x,y}(q_\perp, q_z) = \int d^2 r_\perp \int_0^d dz \, n_{x,y}(r) e^{-iq_\perp \cdot r_\perp} \sin q_z z, \tag{3}$$

where $q_z = m\pi/d$, with m being a positive integer. By substituting the inverse Fourier transforms

$$n_{x,y}(r) = \frac{1}{(2\pi)^2} \int d^2 q_\perp \cdot \frac{2}{d} \sum_{m=1}^{\infty} n_{x,y}(q_\perp, m\pi/d) e^{iq_\perp \cdot r_\perp} \sin \frac{m\pi z}{d} \tag{4}$$

into equation (2), we obtain

$$F_b = \frac{1}{2} K \frac{1}{(2\pi)^2} \int d^2 q_\perp \cdot \frac{2}{d} \sum_{m=1}^{\infty} \left(q_\perp^2 + \left(\frac{m\pi}{d} \right)^2 \right) \sum_{l=x,y} n_l(q_\perp, m\pi/d) n_l(-q_\perp, m\pi/d). \tag{5}$$

Next we consider how particles introduced in the nematic cell deform the director field. We write the surface energy on the particles in the Rapini–Papoular form [39] as

$$F_s = \sum_p \oint_{\Omega_p} d^2 S \, W(s)(\nu(s) \cdot n(s))^2. \tag{6}$$

Here p is the index labelling the particles and Ω_p denotes the surface of the pth particle p. The integral is taken over Ω_p and $d^2 S$ is the surface element. The anchoring strength is given by $W(s)$ and $\nu(s)$ is the unit normal to the surface at the point s. In the case of homeotropic anchoring, $W(s) < 0$ and vice versa for planar anchoring.

We restrict ourselves to the case of weak anchoring on the particle surfaces so that the director field is only slightly deformed by the particles from its ground state (uniform alignment along the z-direction). Then we can safely assume that the director field $n(r)$ is defined throughout the system, even within particles, and continuous so that the Fourier transform (3) is well-defined. Since the surface anchoring energy and the Frank elastic energy are of the order of Wr_0^2 and Kr_0, respectively, with r_0 being the characteristic size of the particle, the condition of weak anchoring is written as $Wr_0/K \ll 1$. A typical value of the Frank elastic constant is $K \sim 10^{-6}$ dyn, and when we consider a micrometre-size droplet ($r_0 \sim 10^{-4}$ cm), the anchoring strength must satisfy $W \ll 10^{-2}$ erg cm^{-2}. In the case of glycerol droplets [14], weak anchoring is safely assumed because W is of the order of 10^{-3}–10^{-4} erg cm^{-2}.

In dealing with the surface energy, we make a gradient expansion of the director field $n(s)$ around the centre of gravity of the particle p, which we will denote by $r^{(p)}$. This treatment is justified when the characteristic size of the particle r_0 is sufficiently smaller than the characteristic length of the elastic distortion in a nematic liquid crystal (in our case, the cell thickness d corresponds to it and $r_0 \ll d$ is required). Since the bulk energy F_b (equations (1) and (2)) contains only terms up to second order in the gradients, it is sufficient to make a

gradient expansion up to second order also for the surface energy F_s. Then the director field can be represented as

$$n(s) = n(r^{(p)}) + (s - r^{(p)})_i \frac{\partial}{\partial r_i^{(p)}} n(r^{(p)})$$

$$+ \frac{1}{2}(s - r^{(p)})_i (s - r^{(p)})_j \frac{\partial}{\partial r_i^{(p)}} \frac{\partial}{\partial r_j^{(p)}} n(r^{(p)}) + \cdots. \tag{7}$$

where $i, j = x, y$ or z and in this subsection summations over x, y and z are implied for repeated indices unless otherwise stated. After some calculations using equation (7), we find

$$\oint_{\Omega_p} \mathrm{d}^2 S\, W(s)(\nu(s) \cdot n(s))^2 \simeq \sum_{l=x,y} \mathcal{A}_{zl}^{(p)} n_l(r^{(p)}) \tag{8}$$

for the pth particle. Here we have defined the operator

$$\mathcal{A}_{kl}^{(p)} = \alpha_{kl}^{(p)} + \beta_{jkl}^{(p)} \frac{\partial}{\partial r_j^{(p)}} + \gamma_{ijkl}^{(p)} \frac{\partial}{\partial r_i^{(p)}} \frac{\partial}{\partial r_j^{(p)}}, \tag{9}$$

with $\alpha_{kl}^{(p)}$, $\beta_{jkl}^{(p)}$ and $\gamma_{ijkl}^{(p)}$ being the tensors characterizing the geometry of the particles defined as [25]

$$\alpha_{kl}^{(p)} = 2 \oint_{\Omega_p} \mathrm{d}^2 S\, W(s)\nu_k(s)\nu_l(s), \tag{10}$$

$$\beta_{jkl}^{(p)} = 2 \oint_{\Omega_p} \mathrm{d}^2 S\, W(s)(s - r^{(p)})_j \nu_k(s)\nu_l(s), \tag{11}$$

$$\gamma_{ijkl}^{(p)} = \oint_{\Omega_p} \mathrm{d}^2 S\, W(s)(s - r^{(p)})_i (s - r^{(p)})_j \nu_k(s)\nu_l(s). \tag{12}$$

We note that in equation (8) we have retained only terms up to second order in the gradients as mentioned above and up to first order in n_x and n_y as in the previous study [25, 30, 36]. Although this truncation allows us to make a completely analytic calculation of the interaction energy and give a contribution which is correct to the leading order in the anchoring strength W, we have to restrict ourselves to a discussion of two-body interaction only. Inclusion of higher-order terms in n_l (third or higher in the Frank elastic energy and second or higher in the anchoring energy) is required to analyse many-body interactions, but it will be almost impossible to give an analytic argument when higher-order terms are incorporated. Here we merely point out that the authors of [26, 27] included second-order terms in the anchoring energy to discuss the effective screening of two-body interaction when the interparticle distance is large enough to accommodate other particles in between.

The surface energy is finally written as

$$F_s = \sum_p \sum_{l=x,y} \mathcal{A}_{zl}^{(p)} n_l(r^{(p)})$$

$$= \sum_p \frac{1}{(2\pi)^2} \int \mathrm{d}^2 q_\perp \cdot \frac{2}{d} \sum_{m=1}^\infty \sum_{l=x,y} n_l(q_\perp, m\pi/d)\mathcal{A}_{zl}^{(p)} \left(e^{iq \cdot r_\perp^{(p)}} \sin \frac{m\pi r_z^{(p)}}{d} \right). \tag{13}$$

Now we proceed to the calculation of the energy associated with the elastic deformation by the particles. The total energy of the system F is the sum of the bulk energy F_b (equation (2)) and the surface energy (equation (13)). We will denote the distortion profile that minimizes the total energy in the presence of particles by $n_{x,y}^{\min}$ which can be determined through the conditions

$$\frac{\delta(F_b + F_s)}{\delta n_{x,y}(q_\perp, m\pi/d)} \bigg|_{n_{x,y}^{\min}} = 0. \tag{14}$$

We find from the calculation of equation (14) that the resultant distortion can be represented as a superposition of those due to one particle, that is, $n_{x,y}^{\min} = \sum_p n_{x,y}^{(p)\,\min}$. Here $n_{x,y}^{(p)\,\min}$ denotes the distortions due to a single particle p, written as

$$n_{x,y}^{(p)\,\min}(q_\perp, m\pi/d) = -\frac{1}{K(q_\perp^2 + (m\pi/d)^2)} \mathcal{A}_{zx,zy}^{(p)} \left(e^{-i q \cdot r_\perp^{(p)}} \sin \frac{m\pi r_z^{(p)}}{d} \right). \tag{15}$$

The total energy can be obtained by substituting $n_{x,y}^{\min}(q_\perp, q_z)$ into $F = F_b + F_s$ and the result is written as

$$F = -\frac{1}{2} \frac{1}{(2\pi)^2} \int d^2 q_\perp \cdot \frac{2}{d} \sum_{m=1}^{\infty} \frac{1}{K(q_\perp^2 + (m\pi/d)^2)}$$

$$\times \sum_p \sum_{p'} \sum_{l=x,y} \mathcal{A}_{zl}^{(p)} \mathcal{A}_{zl}^{(p')} \left(e^{i q \cdot r_\perp^{(pp')}} \sin \frac{m\pi r_z^{(p)}}{d} \sin \frac{m\pi r_z^{(p')}}{d} \right), \tag{16}$$

where $r_\perp^{(pp')} = r_\perp^{(p)} - r_\perp^{(p')}$. We can use the results of the calculations in our previous paper [36] almost directly and obtain

$$F = -\frac{1}{8\pi K} \sum_p \sum_{p'} \sum_{l=x,y} \mathcal{A}_{zl}^{(p)} \mathcal{A}_{zl}^{(p')} [h_1(|r_\perp^{(pp')}|, r_z^{(p)} - r_z^{(p')}) - h_1(|r_\perp^{(pp')}|, r_z^{(p)} + r_z^{(p')})], \tag{17}$$

where we have defined [36]

$$h_1(\xi, \eta) = \frac{1}{\sqrt{\xi^2 + \eta^2}} + \sum_{m=1}^{\infty} \left\{ \frac{1}{\sqrt{\xi^2 + (\eta - 2md)^2}} + \frac{1}{\sqrt{\xi^2 + (\eta + 2md)^2}} - \frac{1}{md} \right\}. \tag{18}$$

2.2. Planar anchoring case

The argument above can be directly applied to a nematic cell with strong planar anchoring on the confining walls. When we take the x-axis parallel to the orientation of planar anchoring, the Frank elastic energy and the surface energy are written as

$$F_b = \frac{1}{2} K \int d^2 r_\perp \int_0^d dz \, \{(\nabla n_y(r))^2 + (\nabla n_z(r))^2\}, \tag{19}$$

$$F_s = \sum_p \sum_{l=y,z} \mathcal{A}_{xl}^{(p)} n_l(r^{(p)})$$

$$= \sum_p \frac{1}{(2\pi)^2} \int d^2 q_\perp \cdot \frac{2}{d} \sum_{m=1}^{\infty} \sum_{l=y,z} n_l(q_\perp, m\pi/d) \mathcal{A}_{xl} \left(e^{i q \cdot r_\perp^{(p)}} \sin \frac{m\pi r_z^{(p)}}{d} \right). \tag{20}$$

Following the same procedures as given in the previous subsection, we obtain

$$F = -\frac{1}{8\pi K} \sum_p \sum_{p'} \sum_{l=y,z} \mathcal{A}_{xl}^{(p)} \mathcal{A}_{xl}^{(p')} [h_1(|r_\perp^{(pp')}|, r_z^{(p)} - r_z^{(p')}) - h_1(|r_\perp^{(pp')}|, r_z^{(p)} + r_z^{(p')})], \tag{21}$$

where the only difference from equation (17) can be found in the indices of the operators $\mathcal{A}$.

3. Discussion

3.1. Interaction energy and self-energy

The resultant free energy of the system, equations (17) and (21), can be rewritten as $F = \sum_{p<p'} U_{pp'} + \sum_p F_p$, where $U_{pp'}$ is the energy of interaction between the pth and

p'th particles and taking into account the double count in the summation we obtain

$$U_{pp'}(\boldsymbol{r}^{(p)}, \boldsymbol{r}^{(p')}) = -\frac{1}{4\pi K} \sum_{l=x,y} \mathcal{A}_{zl}^{(p)} \mathcal{A}_{zl}^{(p')}[h_1(|\boldsymbol{r}_\perp^{(pp')}|, r_z^{(p)} - r_z^{(p')}) - h_1(|\boldsymbol{r}_\perp^{(pp')}|, r_z^{(p)} + r_z^{(p')})]$$

(22)

for the case of homeotropic anchoring on the cell surfaces and

$$U_{pp'}(\boldsymbol{r}^{(p)}, \boldsymbol{r}^{(p')}) = -\frac{1}{4\pi K} \sum_{l=y,z} \mathcal{A}_{xl}^{(p)} \mathcal{A}_{xl}^{(p')}[h_1(|\boldsymbol{r}_\perp^{(pp')}|, r_z^{(p)} - r_z^{(p')}) - h_1(|\boldsymbol{r}_\perp^{(pp')}|, r_z^{(p)} + r_z^{(p')})]$$

(23)

for planar anchoring. $F_{(p)}$ can be called self-energy and is the energy of one particle p. It can also be interpreted as the interaction energy between a particle and confining walls. It is formally written as $F_{(p)}(\boldsymbol{r}^{(p)}) = (1/2)U_{pp'}(\boldsymbol{r}^{(p)}, \boldsymbol{r}^{(p')})|_{\boldsymbol{r}^{(p)}=\boldsymbol{r}^{(p')}}$. $F_{(p)}$ is not well-defined in a naive sense because $h_1(|\boldsymbol{r}_\perp^{(pp')}|, r_z^{(p)} - r_z^{(p')})$ becomes singular when $\boldsymbol{r}^{(p)} = \boldsymbol{r}^{(p')}$. However, we are interested in the dependence of F_p on the particle position $\boldsymbol{r}^{(p)}$ and noticing that $\partial g(\boldsymbol{r}^{(p)} - \boldsymbol{r}^{(p')})/\partial \boldsymbol{r}^{(p)} = -\partial g(\boldsymbol{r}^{(p)} - \boldsymbol{r}^{(p')})/\partial \boldsymbol{r}^{(p)} = \partial g(\boldsymbol{r}^{(p)} - \boldsymbol{r}^{(p')})/\partial (\boldsymbol{r}^{(p)} - \boldsymbol{r}^{(p')})$, with g being an arbitrary function of $\boldsymbol{r}^{(p)} - \boldsymbol{r}^{(p')}$, we find that the first term in equations (17) and (21) is dependent only on $\boldsymbol{r}^{(p)} - \boldsymbol{r}^{(p')}$ and not on the particle position itself. Therefore the first term of equations (17), which contains the singularity, can be safely dropped in the discussion of the self-energy and we are left with

$$F_p(\boldsymbol{r}^{(p)}) = \frac{1}{8\pi K} \sum_{l=x,y} \mathcal{A}_{zl}^{(p)} \mathcal{A}_{zl}^{(p')} h_1(|\boldsymbol{r}_\perp^{(pp')}|, r_z^{(p)} + r_z^{(p')})|_{\boldsymbol{r}^{(p)}=\boldsymbol{r}^{(p')}},$$

(24)

for the case of homeotropic anchoring on the cell surfaces and

$$F_p(\boldsymbol{r}^{(p)}) = \frac{1}{8\pi K} \sum_{l=y,z} \mathcal{A}_{xl}^{(p)} \mathcal{A}_{xl}^{(p')} h_1(|\boldsymbol{r}_\perp^{(pp')}|, r_z^{(p)} + r_z^{(p')})|_{\boldsymbol{r}^{(p)}=\boldsymbol{r}^{(p')}},$$

(25)

for planar anchoring.

3.2. Discussion of the interaction energy and the self-energy—the case of spherical particles

To discuss the implication of the results of the free energy obtained in the previous subsection, we restrict ourselves to the simple cases of spherical particles for clarity in what follows. For spherical particles with radius r_0, it is not a difficult task to calculate the tensors given in equations (10), (11) and (12) and one obtains [25] $\alpha_{kl} = (8\pi W r_0^2/3)\delta_{kl}$, $\beta_{jkl} = 0$ and $\gamma_{ijkl} = \Gamma(\delta_{ij}\delta_{kl} + \delta_{ik}\delta_{jl} + \delta_{il}\delta_{jk})$, where $\Gamma \equiv 4\pi W r_0^4/15$. The operators $\mathcal{A}_{kl}^{(p)}$ in equations (17) and (21) then read

$$\mathcal{A}_{kl}^{(p)} = 2\Gamma \frac{\partial^2}{\partial r_k^{(p)} \partial r_l^{(p)}}$$

(26)

for $k \neq l$. For the case of homeotropic anchoring on the surfaces of the confining walls, equations (22) and (26) yield

$$U_{pp'}(\boldsymbol{r}^{(p)}, \boldsymbol{r}^{(p')}) = \frac{24\Gamma^2}{\pi K} \sum_{m=-\infty}^{\infty} \left[\frac{P_4(\hat{\boldsymbol{\xi}}_1(m) \cdot \boldsymbol{e}_z)}{|\boldsymbol{\xi}_1(m)|^5} + \frac{P_4(\hat{\boldsymbol{\xi}}_2(m) \cdot \boldsymbol{e}_z)}{|\boldsymbol{\xi}_2(m)|^5} \right],$$

(27)

where $\boldsymbol{e}_z$ is the unit vector along the z-direction, $P_4(x) = (1/8)(35x^4 - 30x^2 + 3)$ is the Legendre polynomial of degree 4, and we have defined

$$\boldsymbol{\xi}_1(m) \equiv (r_x^{(p)} - r_x^{(p')}, r_y^{(p)} - r_y^{(p')}, r_z^{(p)} - r_z^{(p')} + 2md),$$

(28)

$$\boldsymbol{\xi}_2(m) \equiv (r_x^{(p)} - r_x^{(p')}, r_y^{(p)} - r_y^{(p')}, r_z^{(p)} + r_z^{(p')} + 2md),$$
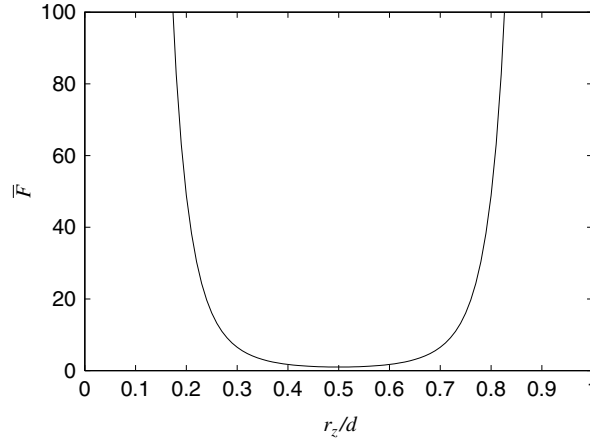
(29)

Figure 1. Reduced self-energy of one particle $\overline{F} = (\pi K/24\Gamma^2)F$ as a function of the particle position r_z.

and $\hat{\xi}_i(m) = \xi_i(m)/|\xi_i(m)|$ for $i = 1$ and 2. From equation (24), the self-energy is calculated as

$$
\begin{aligned}
F_p(\mathbf{r}^{(p)}) &= \frac{12\Gamma^2}{\pi K} \sum_{m=-\infty}^{\infty} \frac{P_4(1)}{|2(r_z^{(p)} + md)|^5} \\
&= \frac{3\Gamma^2}{8\pi K} \sum_{m=-\infty}^{\infty} \frac{1}{|r_z^{(p)} + md|^5}.
\end{aligned}
\tag{30}
$$

We plot the self-energy, equation (30), in figure 1 as a function of the particle position r_z. It is obvious from the up–down symmetry of the system that the profile of the self-energy is symmetric about $r_z/d = 0.5$. It is also found from equation (30) that when the particle is close to one of the confining surfaces, the dominant term in the self-energy is proportional to r_z^{-5} for $r_z \to 0$ and $(d - r_z)^{-5}$ for $r_z \to d$, and therefore the self-energy of a spherical particle diverges as the fifth power of the inverse of the distance to the confining surface.

In the case of planar anchoring we have, from equations (23) and (26),

$$
U_{pp'}(\mathbf{r}^{(p)}, \mathbf{r}^{(p')}) = \frac{\Gamma^2}{\pi K} \sum_{m=-\infty}^{\infty} \left[\frac{24 P_4(\hat{\xi}_1(m) \cdot \mathbf{e}_x)}{|\xi_1(m)|^5} - \frac{2 P_4{}^2(\hat{\xi}_2(m) \cdot \mathbf{e}_x) \cos 2\phi(m)}{|\xi_2(m)|^5} \right],
\tag{31}
$$

where $P_4{}^2(x) = (15/2)(1 - x^2)(7x^2 - 1)$ is the associated Legendre polynomial of degree 4 and order 2, and the azimuthal angle $\phi(m)$ is the angle between the z-axis and $\xi_2(m)$ projected onto the yz plane defined as

$$
\phi(m) \equiv \cos^{-1} \left[\frac{(\hat{\xi}_2(m) \cdot \mathbf{e}_z)}{\sqrt{(\hat{\xi}_2(m) \cdot \mathbf{e}_y)^2 + (\hat{\xi}_2(m) \cdot \mathbf{e}_z)^2}} \right].
\tag{32}
$$

The self-energy is

$$
\begin{aligned}
F_p(\mathbf{r}^{(p)}) &= \frac{\Gamma^2}{2\pi K} \sum_{m=-\infty}^{\infty} \left[-\frac{2 P_4{}^2(0)}{|2(r_z^{(p)} + md)|^5} \right] \\
&= \frac{15\Gamma^2}{64\pi K} \sum_{m=-\infty}^{\infty} \frac{1}{|r_z^{(p)} + md|^5},
\end{aligned}
\tag{33}
$$

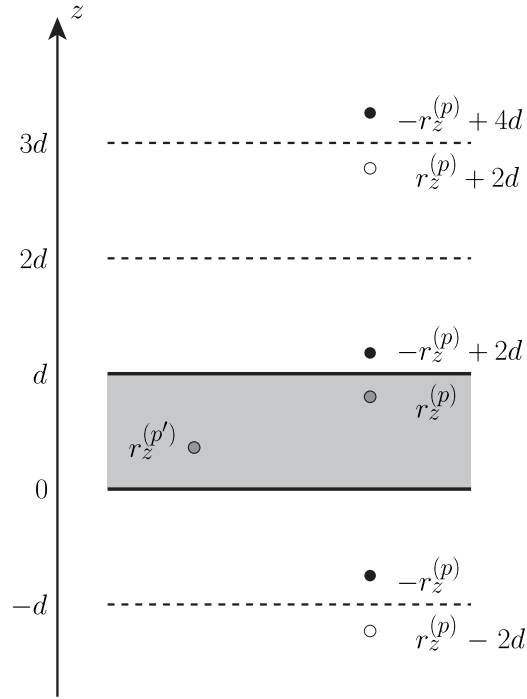which has the same form as equation (30) apart from the prefactor.

Figure 2. Schematic illustration of the mirror images of a particle. Filled (resp. open) circles represent images reflected odd (resp. even) times by the confining surfaces (thick lines). The shaded region is occupied by a nematic liquid crystal. As indicated in the figure, the z-coordinate of the images of the pth particle reflected odd (resp. even) times is $-r_z^{(p)} + 2md$ (resp. $r_z^{(p)} + 2md$).

Equations (27) and (31) clearly indicate that the total interaction is the superposition of quadrupole–quadrupole ones. It has already been found [25] that the interaction between spherical particles in an infinite uniform nematic liquid crystal is a quadrupole–quadrupole one, whose potential is proportional to $P_4(\cos\theta)/r^5$, with r and θ being the interparticle distance and the angle between the direction of the uniform nematic liquid crystal and that of the relative position of the two particles. Notice also that $\boldsymbol{\xi}_1(m)$ and $\boldsymbol{\xi}_2(m)$ represent the distance between the pth particle and a mirror image of the p'th particle reflected even and odd times, respectively, by the confining walls (see figure 2). Therefore the total interaction can be interpreted as the sum of the interactions between one particle and the mirror images of the other particle. In the case of planar anchoring, a different type of interaction proportional to $P_4{}^2(\cos\theta)\cos 2\phi/r^5$ appears (ϕ is the azimuth defined in equation (32)), which is also of quadrupolar–quadrupolar type. This is the interaction between a particle and a mirror image reflected an odd number of times and the difference in the form of the interaction is attributed to the difference in the symmetry of the system. To see that more clearly, we note that the interaction in a homeotropic cell (equation (27)) can also be written as

$$
\begin{aligned}
U_{pp'}(\boldsymbol{r}^{(p)}, \boldsymbol{r}^{(p')}) &= -\frac{\Gamma^2}{\pi K} \sum_{m=-\infty}^{\infty} \sum_{l=x,y} \frac{\partial^4}{\partial r_z^{(p)} \partial r_z^{(p')} \partial r_l^{(p)} \partial r_l^{(p')}} \left[\frac{1}{|\boldsymbol{\xi}_1(m)|} - \frac{1}{|\boldsymbol{\xi}_2(m)|} \right] \\
&= -\frac{\Gamma^2}{\pi K} \sum_{m=-\infty}^{\infty} \frac{\partial^2}{\partial (r_z^{(p)})^2} \left(\frac{\partial^2}{\partial (r_x^{(p)})^2} + \frac{\partial^2}{\partial (r_y^{(p)})^2} \right) \left[\frac{1}{|\boldsymbol{\xi}_1(m)|} + \frac{1}{|\boldsymbol{\xi}_2(m)|} \right],
\end{aligned} \qquad (34)
$$

and the interaction in a planar cell (equation (31)) as

$$U_{pp'}(\boldsymbol{r}^{(p)}, \boldsymbol{r}^{(p')}) = -\frac{\Gamma^2}{\pi K} \sum_{m=-\infty}^{\infty} \sum_{l=y,z} \frac{\partial^4}{\partial_x^{(p)} \partial_x^{(p')} \partial_l^{(p)} \partial_l^{(p')}} \left[\frac{1}{|\boldsymbol{\xi}_1(m)|} - \frac{1}{|\boldsymbol{\xi}_2(m)|} \right]$$

$$= -\frac{\Gamma^2}{\pi K} \sum_{m=-\infty}^{\infty} \frac{\partial^2}{\partial (r_x^{(p)})^2} \left[\left(\frac{\partial^2}{\partial (r_y^{(p)})^2} + \frac{\partial^2}{\partial (r_z^{(p)})^2} \right) \frac{1}{|\boldsymbol{\xi}_1(m)|} \right.$$

$$\left. - \left(\frac{\partial^2}{\partial (r_y^{(p)})^2} - \frac{\partial^2}{\partial (r_z^{(p)})^2} \right) \frac{1}{|\boldsymbol{\xi}_2(m)|} \right]. \tag{35}$$

The presence of rotational symmetry around the z-axis in a homeotropic cell (note that the z-axis is parallel to the director) is clearly reflected in equation (34), while in a planar cell the confining walls do not allow rotational symmetry around the director (along the x-axis). Therefore the two directions perpendicular to the director, y and z, are not equivalent as in a homeotropic cell, which results in different forms of the interaction as can be seen in equation (35).

One can also find that the self-energy, equations (30) and (33), can be regarded as the interaction energy between a particle and its mirror images. Note that the distance between a particle and one of its images reflected an even number of times by the confining walls (open circles in figure 2) does not depend on the position of the particle. Therefore only the interactions between the particle and its images reflected odd times contribute to the self-energy, which is manifested in equations (30) and (33) (notice that the distance between the particle and its image is $|2(r_z^{(p)} + md)|$).

3.3. Profiles of the interaction energy and the self-energy

It will be instructive to present the profile of the free energy and the resultant interaction of two particles, which is the aim of this subsection.

3.3.1. Homeotropic alignment. In the case of homeotropic alignment, the interaction energy (equation (22) for general cases or equation (27) for spherical particles) depends on $|r_\perp^{(pp')}|$, $r_z^{(p)}$ and $r_z^{(p')}$, and we show in figure 3 the free energy of a nematic cell containing two particles as a function of the position of one particle (labelled by p), while the position of the other particle (labelled by p') is fixed to $r_z^{(p')}/d = 0.5$, 0.3 or 0.25. The total energy is the sum of the interaction energy $U_{pp'}$ and the self-energies F_p and $F_{p'}$, and in figure 3 we plot the reduced free energy defined as

$$\overline{F}(|r_\perp^{(pp')}|, r_z^{(p)}) \equiv \frac{\pi K}{24\Gamma^2} \{ U_{pp'}(|r_\perp^{(pp')}|, r_z^{(p)}) + F_p(r_z^{(p)}) - F_p(r_z^{(p)} = 0.5d) \}, \tag{36}$$

where the self-energy of the fixed particle $F_{p'}$ is not included, and $\overline{F}(|r_\perp^{(pp')}| \to \infty, r_z^{(p)} = 0.5d) = 0$. In figure 3(a), for reference, we also plot the interaction energy in an infinite nematic medium, $\overline{F} = P_4(\hat{\boldsymbol{r}}^{(pp')} \cdot \boldsymbol{e}_z)/|\boldsymbol{r}^{(pp')}|^5$.

We find from figure 3 that the profile of the total free energy of a confined system is almost the same as that in an infinite medium (figure 3(a)) when $|r^{(pp')}| \lesssim 0.2$. While they are significantly different when $|r^{(pp')}|$ becomes larger or when the non-fixed particle is close to one of the confining walls (i.e. $r_z^{(p)}/d \to 0$ or 1), in which cases one observes that the self-energy, or the interaction with confining walls, dominates the free energy. In figures 3(b) and (c), we also observe the presence of saddle points (in figure 3(b), $r_\perp^{(pp')}/d \simeq 0.55$ and in figure 3(c), $r_\perp^{(pp')}/d \simeq 0.8$) in the free energy landscape. In those cases, the non-fixed particle
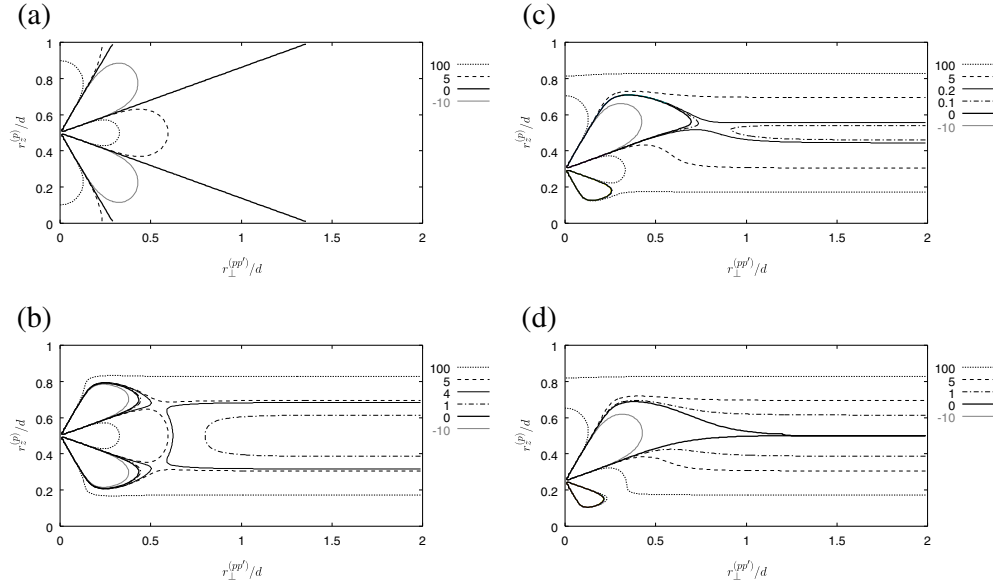
Figure 3. Contour plots of the reduced free energy of the system $\overline{F} = (\pi K/24\Gamma^2)F$ as a function of the position of one particle in the case of homeotropic alignment. (a) The interaction energy in an infinite nematic medium (for reference). (b) $r_z^{(p')} = 0.5d$. (c) $r_z^{(p')} = 0.3d$. (d) $r_z^{(p')} = 0.25d$.

cannot approach the fixed one when $r_\perp^{(pp')}$ is larger than that of the saddle point(s). While we find from the self-energy (figure 1) that the most stable position of one particle is $z = 0.5d$, the total energy of the system reveals that particles cannot aggregate on a single plane $z = 0.5d$ solely by the elasticity-mediated interaction. Therefore the superstructure of particles in a homeotropically aligned cell cannot be one layer placed at $z = 0.5d$. On the other hand, such a saddle point is absent in figure 3(d) and the lines corresponding to $\overline{F} = 0$ go to infinity in contrast to figures 3(b) and (c), which demonstrates that the non-fixed particle feels attractive force from the fixed particle even when the distance between two particles are large enough. This observation indicates that particles may aggregate to form a multi-layered structure.

3.3.2. Planar alignment. A nematic cell with planar alignment lacks rotational symmetry around the z-axis, and the interaction energy then depends on $r_x^{(pp')}$, $r_y^{(pp')}$, $r_z^{(p)}$ and $r_z^{(p')}$. In figure 4, we plot the total energy of the system as defined in equation (36) with one particle fixed. Two planes of symmetry, $r_x^{(pp')} = 0$ and $r_y^{(pp')} = 0$, are still present in the system and it is sufficient to present the plot in a space specified by $r_x^{(pp')} \geqslant 0$, $r_y^{(pp')} \geqslant 0$ and $0 < r_z^{(p)}/d < 1$. Notice that figure 4(a) showing the interaction energy in an infinite medium can be obtained by simply rotating figure 3(a) around the z-axis (with an appropriate redefinition of the coordinate system). As in the case of a homeotropically aligned cell discussed previously, the energy landscape is quite sensitive to the position of the fixed particle as can be seen from figures 4(b)–(d). We also find, by comparing figures 4(b)–(d) with figure 4(a), that when the distance between particles is large enough, the self-energy of the non-fixed particle dominates the total energy. As expected from the interaction energy in an infinite system (figure 4(a)), the non-fixed particle can approach the fixed one not along the x- or y-axis but along an oblique direction in the cases of figures 4(b) and (c). However, from figure 4(d), we observe
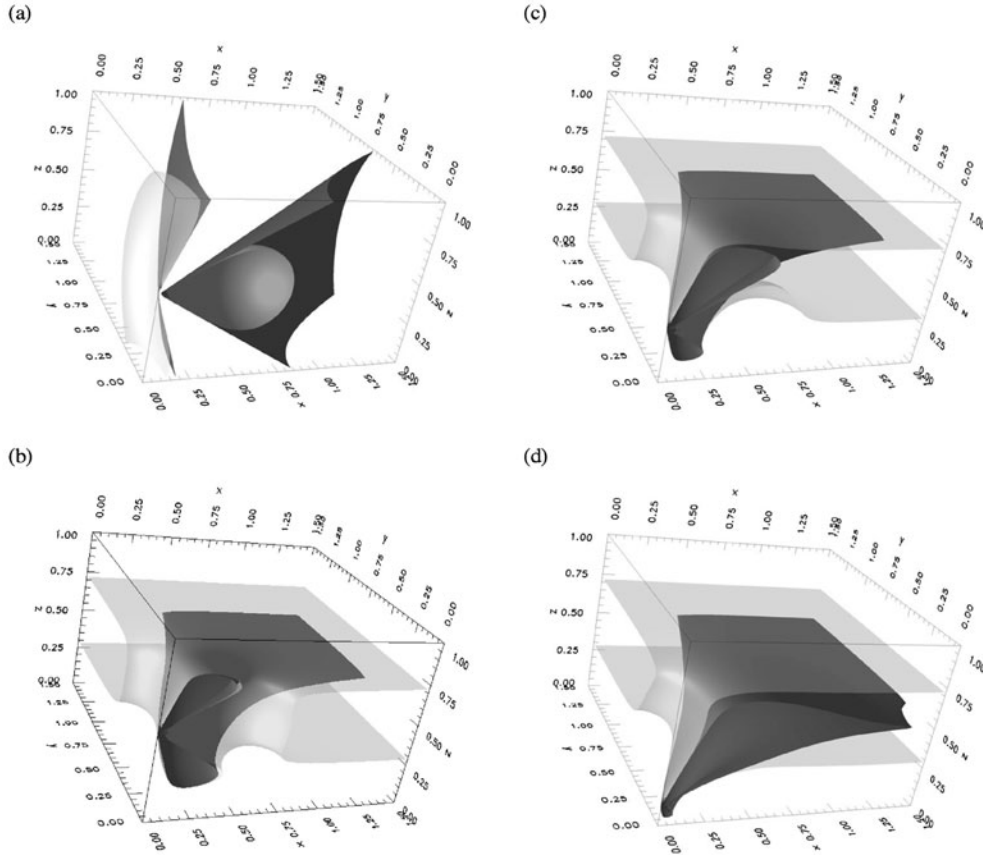
Figure 4. Isosurface plots of the free energy in the case of planar alignment along the x-direction. (a) The interaction energy in an infinite nematic medium (for reference). (b) $r_z^{(p')} = 0.5d$. (c) $r_z^{(p')} = 0.3d$. (d) $r_z^{(p')} = 0.1d$. The opaque light grey isosurface corresponds to $\overline{F} = (\pi K/24\Gamma^2)F = 5$ and the dark grey one to $\overline{F} = 0$. The labels x, y and z in the figures imply $r_x^{(pp')}/d$, $r_y^{(pp')}/d$ and $r_z^{(p)}/d$ respectively.

that the non-fixed particle does not feel repulsion when it approaches the fixed one along the x-direction, and this observation is quite similar to that in figure 3(d).

4. Conclusion

We investigated theoretically how the interaction of particles immersed in a nematic liquid crystal cell is affected by the confining walls that impose strong anchoring. We obtained the analytic form of the interaction energy when the anchoring of the particle surfaces is weak enough. We showed that the resultant form of the interaction energy is regarded as the interaction of one particle with an infinite array of the mirror images of the other. The self-energy, or the interaction of one particle with the confining walls, can also be interpreted along the same lines, that is, interaction with an infinite array of its images. The method of images, which belongs to an elementary course in electrostatics, has been successfully used in the field of liquid crystals to understand the interaction between a line defect and a flat wall [37, 38]

(or a point defect and a circular bubble in a two-dimensional film [38]). So far as we know, however, this paper is the first to point out that the method of images can also be applied to the theoretical investigation of the elasticity-mediated interaction of particles in a liquid crystal. We also presented the formula for the interaction energy and the self-energy for the simple case of spherical particles in nematic cells with strong homeotropic or planar anchoring on the confining walls. While the interaction in a homeotropic cell is simply the superposition of the quadrupole–quadrupole interactions in an infinite medium, in a planar cell a different interaction, which is still of the quadrupole–quadrupole type, appears between a particle and its image reflected an odd number of times due to the difference in the symmetry of the cell. From the landscape of the interaction energy and the self-energy, we found that the energy landscape is sensitive to the distance of a particle to the confining walls, which may affect the kinetics of particle aggregation.

We notice that our interaction energy may be used as an effective potential in molecular dynamics [40] or Brownian dynamics simulations for investigating the formation of superstructures in liquid crystal colloids after introducing an appropriate truncation in the infinite series appearing in the formulae of the potential. We believe that the combination of our theoretical results with simulation techniques for particle systems will provide a powerful tool for the understanding of not only the equilibrium structure but also the kinetic process of structure formation in a nematic cell containing particles.

Finally, a few remarks about the experimental test of the present predictions may be in order. The practical relevance of the above theory, presumably over the previous theoretical treatments, lies in the realistic nature of the model assuming the presence of the confining walls as well as the rich analytical predictions it can make. Although it has been commonly understood that the strength and symmetry of the interparticle interactions are the key to understand the variety of liquid crystal colloidal structures so far observed, quantitative observation of the interparticle forces has been rare. If the refractive indices of the particle and the host liquid crystal can be taken as sufficiently different from each other, it is now possible to optically grab and translate the particle, and to measure precisely the force acting on the particle with pN precision by means of the so-called optical tweezer; a position-controlled laser beam focused on the particle. By using dual optical tweezers, it should be possible to directly examine the specific predictions of the present theory in great detail. We hope that our theoretical arguments presented here will promote experimental studies concerning the elasticity-mediated interaction in a liquid crystal.

References

[1] Poulin P, Raghunathan V A, Richetti P and Roux D 1997 *J. Physique* II **4** 1557
    Raghunathan V A, Richetti P and Roux D 1996 *Langmuir* **12** 3789
    Raghunathan V A, Richetti P, Roux D, Nallet F and Sood A K 1996 *Mol. Cryst. Liq. Cryst.* **288** 181
    Raghunathan V A, Richetti P, Roux D, Nallet F and Sood A K 2000 *Langmuir* **16** 4720
[2] Poulin P, Stark H, Lubensky T C and Weitz D A 1997 *Science* **275** 1770
[3] Poulin P 1999 *Curr. Opin. Colloid Interface Sci.* **4** 66
[4] Zapotocky M, Ramos L, Poulin P, Lubensky T C and Weitz D A 1999 *Science* **283** 209
[5] Meeker S P, Poon W C K, Crain J and Terentjev E M 2000 *Phys. Rev.* E **61** R6083
[6] Anderson V J, Terentjev E M, Meeker S P, Crain J and Poon W C K 2001 *Eur. Phys. J.* E **4** 11
    Anderson V J and Terentjev E M 2001 *Eur. Phys. J.* E **4** 21
[7] Yamamoto J and Tanaka H 2001 *Nature* **409** 321
[8] Russel W B, Saville D A and Schowalter W R 1995 *Colloidal Dispersions* (Cambridge: Cambridge University Press)
[9] Poulin P, Cabuil V and Weitz D A 1997 *Phys. Rev. Lett.* **79** 4862
[10] Poulin P and Weitz D A 1998 *Phys. Rev.* E **57** 626

[11] Loudet J-C, Barois P and Poulin P 2000 *Nature* **407** 611
[12] Poulin P, Francès N and Mondain-Monval O 1999 *Phys. Rev.* E **59** 4384
[13] Mondain-Monval O, Dedieu J C, Gulik-Krzywicki T and Poulin P 1999 *Eur. Phys. J.* B **12** 167
[14] Nazarenko V G, Nych A B and Lev B I 2001 *Phys. Rev. Lett.* **87** 075504
[15] Cluzeau P, Poulin P, Joly G and Nguyen H T 2001 *Phys. Rev.* E **63** 031702
[16] Cluzeau P, Joly G, Nguyen H T and Dolganov V K 2002 *JETP Lett.* **75** 482
[17] Loudet J C and Poulin P 2001 *Phys. Rev. Lett.* **87** 165503
[18] Lev B I, Nych A, Ognysta U, Reznikov D, Chernyshuk S and Nazarenko V 2002 *JETP Lett.* **75** 322
[19] Yamamoto T, Yamamoto J, Lev B I and Yokoyama H 2002 *Appl. Phys. Lett.* **81** 2187
[20] Lopatnikov S L and Namiot V A 1978 *Sov. Phys.–JETP* **48** 180
[21] Ramaswamy S, Nityananda R, Raghunathan V A and Prost J 1996 *Mol. Cryst. Liq. Cryst.* **288** 175
[22] Ruhwandl R W and Terentjev E M 1997 *Phys. Rev.* E **55** 2958
[23] Lubensky T C, Pettey D, Currier N and Stark H 1998 *Phys. Rev.* E **57** 610
[24] Stark H, Stelzer J and Bernhard R 1999 *Eur. Phys. J.* B **10** 515
[25] Lev B I and Tomchuk P M 1999 *Phys. Rev.* E **59** 591
[26] Chernyshuk S B, Lev B I and Yokoyama H 2001 *Sov. Phys.–JETP* **93** 760
[27] Lev B I, Chernyshuk S B, Tomchuk P M and Yokoyama H 2002 *Phys. Rev.* E **65** 021709
[28] Turner M S and Sens P 1997 *Phys. Rev.* E **55** R1275
     Sens P, Turner M S and Pincus P 1997 *Phys. Rev.* E **55** 4394
     Sens P and Turner M S 1997 *J. Physique* II **7** 1855
     Turner M S and Sens P 1998 *Phys. Rev.* E **57** 823
[29] Groenwold J and Fredrickson G H 2001 *Eur. Phys. J.* E **5** 171
[30] Fukuda J, Lev B I and Yokoyama H 2002 *Phys. Rev.* E **65** 031710
[31] Borštnik A, Stark H and Žumer S 1999 *Phys. Rev.* E **60** 4210
     Borštnik A, Stark H and Žumer S 2000 *Phys. Rev.* E **61** 2831
[32] Galatola P and Fournier J-B 2001 *Phys. Rev. Lett.* **86** 3915
     Fournier J-B and Galatola P 2002 *Phys. Rev.* E **65** 032702
[33] Stark H 2002 *Phys. Rev.* E **66** 041705
[34] Pettey D, Lubensky T C and Link D 1998 *Liq. Cryst.* **25** 579
[35] Patrício P, Tasinkevych M and Telo da Gama M M 2002 *Eur. Phys. J.* E **7** 117
     Tasinkevych M, Silvestre N M, Patrício P and Telo da Gama M M 2002 *Eur. Phys. J.* E **9** 341
[36] Fukuda J, Lev B I, Aoki K M and Yokoyama H 2002 *Phys. Rev.* E **66** 051711
[37] de Gennes P G and Prost J 1993 *The Physics of Liquid Crystals* 2nd edn (Oxford: Oxford University Press)
[38] Chandrasekhar S 1992 *Liquid Crystals* 2nd edn (Cambridge: Cambridge University Press)
[39] Rapini A and Papoular M 1969 *J. Phys. Coll.* **30** C4–54
[40] Aoki K M, Lev B I and Yokoyama H 2001 *Mol. Cryst. Liq. Cryst.* **367** 537
     Lev B I, Aoki K M, Tomchuk P M and Yokoyama H 2003 *Condens. Matter. Phys.* **6** 169
     In these papers, the authors use effective interaction potential in an infinite nematic liquid crystal